A Doppler Radar Study of Convective Draft Lengths over Darwin, Australia

Nicholas K. H. Yeung,[a,b] Steven C. Sherwood,[a,b] Alain Protat,[c,b] Todd P. Lane,[d,b] and
Christopher Williams[e]

[a] Climate Change Research Centre, University of New South Wales, Sydney, Australia
[b] ARC Centre of Excellence for Climate Extremes, University of New South Wales, Sydney, Australia
[c] Bureau of Meteorology, Melbourne, Australia
[d] University of Melbourne, Melbourne, Australia
[e] NOAA, University of Colorado Boulder, Boulder, Colorado

ABSTRACT: Data from an upward-pointing wind profiler radar pair at Darwin in tropical Australia are used to determine the characteristics of individual convective up- and downdrafts observed at the site. Drafts are identified as vertically contiguous regions of instantaneous upward or downward motion exceeding $0.2\,\mathrm{m\,s^{-1}}$. Most updrafts and downdrafts found are less than 2 km in vertical extent, and updrafts exceeding 5 km in vertical length carry no more than 33% of the total upward mass flux. Updraft length correlates positively with rain rates, and on very high rain rates (greater than $20\,\mathrm{mm\,h^{-1}}$), average updraft lengths are ~5 km. Typical peak updraft velocities increase from ~$2.5\,\mathrm{m\,s^{-1}}$ for the smallest to ~$4\,\mathrm{m\,s^{-1}}$ for the largest drafts, while those for downdrafts remain ~$2\,\mathrm{m\,s^{-1}}$ regardless of size. These results are broadly consistent with other numerical modeling studies, but contrast with the common view of deep convection as being dominated by continuous, deep drafts.

KEYWORDS: Australia; Updrafts/downdrafts; Wind profilers

1. Introduction

Cumulus convection is a vertical mixing process that spans the troposphere in the tropics and often in midlatitudes. It is typically thought of as consisting of continuous, entraining vertical plumes that individually extend through the troposphere, as opposed to incoherent upward convective activities in smaller scales. This picture dates back to the pioneering work of Riehl and Malkus (1958) who argued, in contrast to earlier ideas (Scorer and Ludlam 1953), that the vertical profile of equivalent potential temperature implied direct transport of air from near the surface to the upper troposphere in undilute "hot towers." Their argument ignored the important role of the latent heat of freezing in heating updrafts (Fierro et al. 2012), but the idea of deep, sometimes weakly entraining plumes continues to hold sway and play a prominent role in many deep convective parameterizations for global models (Arakawa 2004; Yano 2014).

Numerical simulations of convection in small domains, however, do not show continuous, deep undiluted plumes playing a significant role at least when deep convection is not strongly organized (Khairoutdinov and Randall 2006; Romps and Kuang 2010). Moreover, detailed analysis of updrafts in such simulations shows that upward motions tend to occur in compact thermals typically of order 1 km in size (Carpenter et al. 1998; Sherwood et al. 2013; Hernandez-Deckers and Sherwood 2016), with essentially no deep coherent updrafts. This conclusion is also supported by aircraft observations of continental small or congestus cumulus (Blyth et al. 1988; French et al. 1999; Damiani and Vali 2007; Blyth et al. 2005; Yang et al. 2016).

Information on highly organized convection is harder to come by. A large-eddy simulation of one of the consistently strongest observed thunderstorms, the Hector over the Tiwi islands north of Australia, produced thousands of small thermal-like drafts similar to the previous studies. However it also eventually produced two deep plumes that carried most of the total upward mass transport (Dauhut et al. 2016). Draft length in numerical simulations may also decrease with increasing resolution (Bryan et al. 2003). Similarly, a detailed analysis of a multicellular thunderstorm over Florida found that upward mass transport was dominated by smaller drafts of less than 5 km (Yuter and Houze 1995a). On the other hand, highly organized severe storms in the subtropics and midlatitudes can produce coherent updrafts and downdrafts via mesoscale dynamical mechanisms (Rotunno et al. 1988). Using a series of axisymmetric numerical cloud simulations, a recent study suggests that in a dry environment, a small initial cloud radius would produce an isolated rising thermal, while a moderate-to-large radius would lead to a succession of thermal pulses (Peters et al. 2020). In contrast, a moderate-to-large radius in a moist environment would support plume-like behavior. Thus, while "hot towers" may dominate in some extreme forms of convection, such storms are not necessarily typical of warm-season convection and it remains uncertain how common deep convective drafts are in nature.

Indirect evidence can be brought to bear, such as stable isotopes of water vapor which are less depleted in the upper troposphere than predicted by an adiabatic calculation, consistent with a short vertical mixing length and suggesting that undilute transport from low levels is rare (Sherwood and Risi 2012). Similarly, profiles of chemical constituents in the upper troposphere indicate that air there has been out of contact with the surface for many days on average (Luo et al. 2018). These
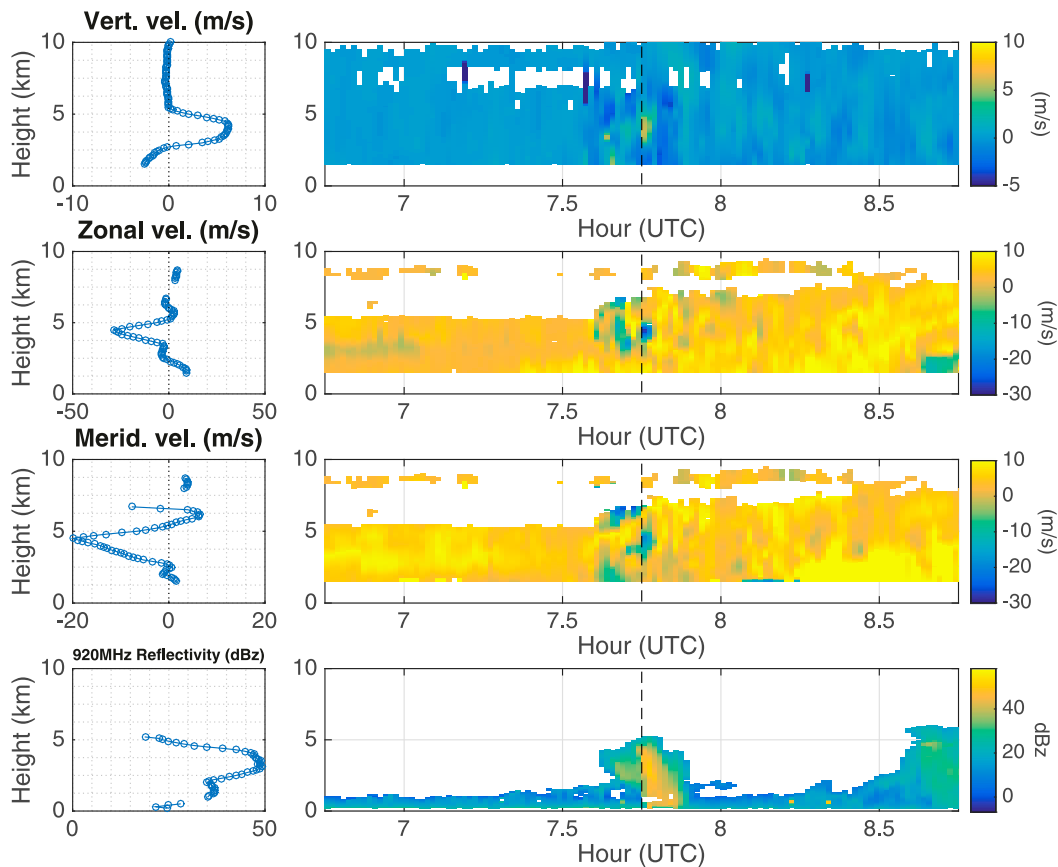
Centre @ 4km, Draft Length = 2.6km, 02/FEB/2017

FIG. 1. A sample of upward, zonal, and meridional velocity at the time where an updraft or downdraft is detected. The white areas in the right column are missing values. The 920-MHz reflectivity from which rain fluxes are estimated is also shown (note that the surface rain rate should be taken from the estimate nearest to the surface). The line plots in the left column correspond to the time of the vertical dashed line in the right column.

results provide further evidence against widespread undilute ascent, and moreover show that this aspect of convective behavior matters for atmospheric chemistry, among other likely ramifications. But the results could be explained either by short mixing lengths or by highly entraining deep drafts. Direct evidence of vertical updraft scales over a large sample of atmospheric conditions, which is needed to properly constrain convective theories or parameterizations, is lacking.

A key platform for studying storm morphology is radar. Most radars look quasi-horizontally and measure large (raining) hydrometeors, and sometimes the horizontal wind, although a few studies have obtained vertical velocities. Standard radars often show vertically extensive regions of backscatter from rain, graupel or other large hydrometeors, but this does not mean the wind field itself is vertically continuous, especially since the updraft and precipitation distributions do not correspond as tightly as might be expected (Yuter and Houze 1995b). Indeed by eye one can sometimes see isolated towering cumulus reach through most of the troposphere as a coherent column, even though evidence indicates that the updrafts within will be sporadic and compact.

Deep clouds can result from a sequence of small thermals rising along the same path (e.g., French et al. 1999).

At Darwin in Australia's Northern Territory there is an upward-looking wind profiler radar pair that measures air and hydrometeor vertical velocities. Past studies have used this radar to examine mass fluxes (Kumar et al. 2015). Schumacher et al. (2015) examined vertical velocities at the same site (Darwin) as the present study. In deep convection they reported updrafts of up to $18\,\mathrm{m\,s}^{-1}$ peaking in the upper troposphere, with weaker velocities for other cloud types, and found statistics were insensitive to the phase of the monsoon-break cycle. They did not, however, examine the vertical coherence of the motions or scale of drafts. Another study using a wind profiler located in Oklahoma (Giangrande et al. 2013) examined this, and found a median updraft and downdraft length of only 1.5–2 km and 90th percentile length of 4 km. Our study has similar aims as Giangrande et al. (2013) but in the tropics. Past studies have reported similar storm structures in mesoscale convective systems (MCSs) across both midlatitude and tropical sites (Oklahoma and Manaus, Brazil), although with

stronger up- and downdrafts in the midlatitude storms (Wang et al. 2019), but again did not examine draft lengths. Here, we use a long time series from the Darwin radar to explore how often extensive plumes of upward motion occur versus compact thermals. We also stratify results by rain rate to test the hypothesis that upward motions become more plume-like in stronger convection.

2. Methods

Over the Darwin wet seasons (October–April) from 2002 to 2012, 1019 days of data collected by a 50- and 920-MHz wind profiler pair were used in this study. It has a temporal resolution of 1 min and vertical spatial resolution of 100 m, with the beamwidths being 3° and 9° for the 50- and 920-MHz profilers, respectively. The Darwin wind profiler radar pair estimate in-cloud velocity by Doppler returns. It is more accurate than other remote sensing methods, such as the dual-Doppler radar techniques (e.g., Collis et al. 2013). However, measurements are limited to a single air column, but taken frequently in time. Vertical velocity computation from the 50- and 920-MHz beams and the full description of the wind profiler setting can be found in Williams (2012).

The 50-MHz profiler directly measures the vertical velocity of air parcels through Bragg scatter from ambient air, but also observes Rayleigh scatter from falling hydrometeors. To avoid observed air velocity being biased downward by hydrometeors, signals from these two scattering processes need to be separated. Since the 920-MHz profiler is mainly sensitive to hydrometeor returns, its spectra are used to remove the Rayleigh scattering signal from the 50-MHz spectra (Williams 2012). The resulting 50-MHz signal is then further processed by the standard wind profiling processing technique described in Carter et al. (1995). The accuracy of vertical air velocity derived from this dual-frequency spectral processing has been estimated as better than $0.2\,\mathrm{m\,s^{-1}}$ (Protat and Williams 2011; Williams 2012).

Over the range of 1.7–17 km in altitude, vertical air velocity measured by the profiler pair is interpolated onto a vertical grid of 100-m interval. Due to reducing sensitivity and increasing beamwidth with height, quality data should be limited to heights below 11 km (May and Rajopadhyaya 1999). As the UHF and VHF radars have the sensitivity to detect vertical velocity in higher altitudes, further examination of our data suggests raising the limit to below 15 km.

Here we present the criteria for detecting updrafts and downdrafts from the wind profiler pair. An algorithm is developed to detect and pick out sections of wind profiles from the available data. For simplicity, we did not apply any time-related criteria in the algorithm. Instead, it is run through individual vertical profiles for every increment in time, as if every profile is independent of each other. This does not ensure that every detection is a distinct draft but should produce statistics that are representative of the total area covered by drafts of any given size or type.

The criteria for an updraft or downdraft are as follows:

1) Updrafts and downdrafts are explicitly defined as a section of continuous upward or downward airflow. Taking upward
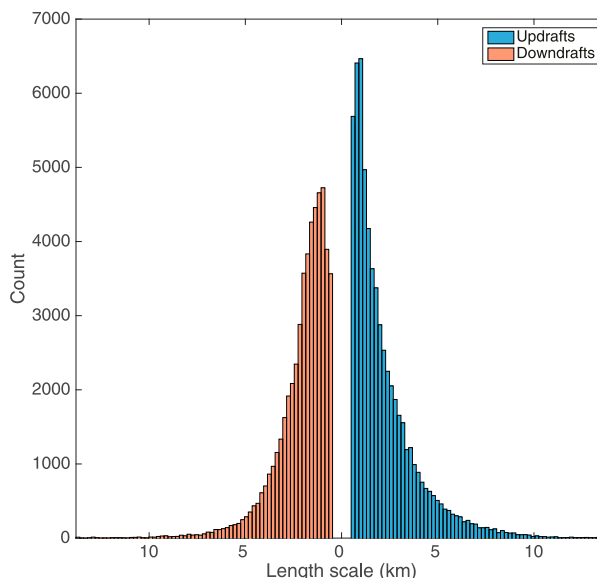

FIG. 2. Number of updrafts and downdrafts in various lengths. Updrafts are shown in blue as positive values, and downdrafts are shown in orange as negative values. Bins are 0.2 km.

as positive, they must have consecutive velocity values over $0.2\,\mathrm{m\,s^{-1}}$ in magnitude, and contain velocities above $1.5\,\mathrm{m\,s^{-1}}$ in magnitude in at least two intervals. Since the velocities of most mesoscale (stratiform) up- and downdrafts are less than $1\,\mathrm{m\,s^{-1}}$ (Knupp and Cotton 1985), the requirement that drafts must reach over $1.5\,\mathrm{m\,s^{-1}}$ should be eliminating nearly all mesoscale drafts.

2) The magnitude of first (bottommost) and last (uppermost) velocities of an updraft or downdraft must be below $5\,\mathrm{m\,s^{-1}}$. This is to avoid artifacts with sharp increases in velocity from less than 0.2 to over $5\,\mathrm{m\,s^{-1}}$ within 100 m. Such an increase is unrealistic and could be due to instrumental error. This removes 47% of data selected from criterion 1, due to the presence of numerous, small blips of reported high velocity that meet criterion 1 but are clearly not legitimate convective drafts.

3) Change in velocity across every 100-m interval must be below $5\,\mathrm{m\,s^{-1}}$. Again, this is to avoid unrealistic data. This criterion further removes 1.6% of data (14% if without criterion 2).

4) A single updraft or downdraft must have a minimum vertical length of at least 500 m. This is because we want to focus on long and consistent updrafts or downdrafts. If this vertical length limit is shortened, the resulting data may be susceptible to the effects of turbulence.

5) Detection is limited to below 15 km in altitude, since the data above this height often exhibit unrealistic or inconsistent behavior.

In total, by applying the above criteria, we detected 61 376 updrafts and 53 038 downdrafts. Out of 1019 days of data with 1-min temporal resolution and 15 km in vertical extent, this corresponds to 4.2 updraft detections and 3.6 downdraft detections per 100 soundings. Since large drafts could be
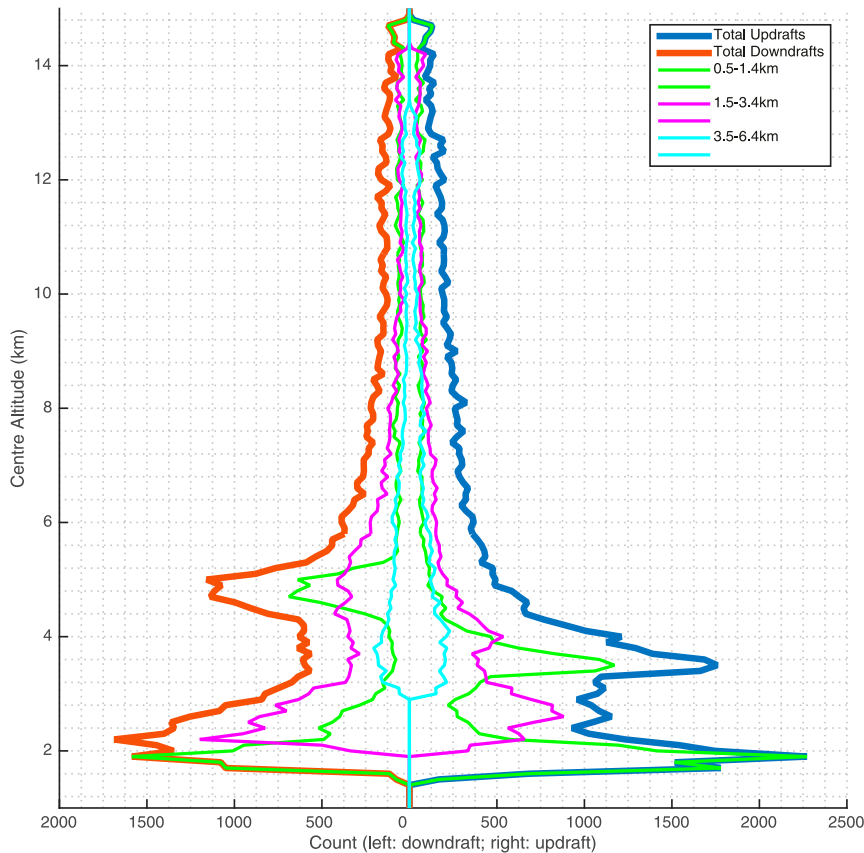
FIG. 3. Number of updrafts and downdrafts vs 100-m height bin. Total up- and downdrafts are shown in blue and orange, respectively. Green curves show only drafts in the 0.5–1.4-km length range, magenta shows only drafts in the 1.5–3.4-km length range, and cyan shows only drafts in the 3.5–6.4-km length range.

detected in more than one successive sounding, the number of actual drafts seen will be somewhat less than this. About 12% of updrafts are sampled from soundings that individually contain multiple distinct updrafts; this figure is 7% for downdrafts. Our method does not identify or remove overlapped cores, but treats them as one single draft as long as they fit the selecting criteria.

A limitation of this approach is that since instantaneous upward-looking data are used, tilted drafts may be incompletely seen. In principle this could bias our results toward smaller drafts. Inspection of selected time–height series did not suggest a prevalence of evident tilted structures, so it does not appear that our results would be significantly affected by such structures. Tilting in a direction transverse to the storm motion past the radar cannot be ruled out, but would not be detectable from the available data. However, we do not expect drafts to be preferentially tilted perpendicular to winds. It will turn out that most of our draft lengths are too small to be consistent with a tilted draft of the expected width (at least a few kilometers), minimizing the likely role of tilting; and as will be seen, our results are consistent with numerical model simulations (see section 1) showing that most updrafts occur in thermals with length-to-height ratios of order unity.

An example sequence of data is shown in Fig. 1. This figure includes vertical velocity, zonal and meridional velocity and reflectivity, during a period in which an updraft of 2.6 km in length was detected. Convective activity is evident. Upward, zonal, and meridional velocities all peak at ~5 km, coinciding with high reflectivity. As will be shown further in section 3, small drafts are quite typical.

In section 3c, draft relationship with rain rates is discussed. Rain rates are derived from the reflectivity of the 920-MHz profiler, which is sensitive to hydrometeor. The conversion follows a locally derived relationship during the wet season in Darwin:

$$R = 0.017 \times (10^{Zh/10})^{0.72}, \tag{1}$$

where R is the rain rate (mm h^{-1}) and Zh is the reflectivity of the 920-MHz profiler vertical beam at 200-m range (dBZ). Equation (1) was obtained by the Australian Bureau of Meteorology from radar and disdrometer observations using the method described in section 3.2 of Jackson et al. (2021), except using S-band reflectivities, which should be closer to those from the Doppler radar used in the present study. The rain rate associated with any detected draft has been averaged

over ± 30 min of the time of detection. This is to smooth out any artifacts and create a more reliable representation of convective activities.

3. Results

The numbers of updrafts and downdrafts both decrease approximately exponentially with increasing length scale (Fig. 2). Updrafts and downdrafts between 0.9 and 1.1 km in length occur most frequently, comprising 6466 updrafts (~11% of all updrafts), and 4725 downdrafts (~9% of all downdrafts). Coincidentally, the largest updraft and downdraft detected are both 13.8 km in length.

The median updraft length is 1.6 km, with the 90th percentile length being 4.5 km. For downdrafts, the median and 90th percentile length are 1.7 and 3.7 km, respectively. Interestingly, these values are similar to the statistics of horizontal draft size obtained in midlatitude cases by Giangrande et al. (2013).

The prevalence of updrafts over downdrafts is expected since there should be net upward motion in regions of rainfall and latent heat release. The sizeable number of downdrafts is consistent with previous modeling and observational studies (Xu and Randall 2001), and the exponentially decreasing size distribution and small average size are consistent with that reported in a large number of thermals tracked by Hernandez-Deckers and Sherwood (2016).

a. Distribution across altitudes

How updrafts and downdrafts are distributed across altitudes is a subject of interest. In Fig. 3, histograms of draft midpoint altitude are plotted separately for up- and downdrafts, separately for several length categories. The most common updraft altitude is at around 2 km, and these are heavily dominated by small updrafts (lengths from 0.5 to 1.4 km). There is a corresponding peak in small downdrafts at these altitudes. These low peaks could be due to the fact that there is often turbulence in the boundary layer.

There are also peaks in detected updrafts and downdrafts at 3.5 and 5 km, respectively, again coming from the smallest drafts. Between the peaks dominated by small drafts at 2 and 3.5 km for updrafts and at 2 and 5 km for downdrafts, drafts in the middle size category (1.5–3.4 km) take over and have the highest proportion. Since we are using the midpoint of drafts to produce Fig. 3, this suggests that under an altitude of ~3 km for updrafts and ~4 km for downdrafts, drafts in lengths between 0.5 and 3.4 km usually share a common starting altitude at about 2 km. Above 4 km for updrafts and 5 km for downdrafts, middle-sized drafts (1.5–3.4 km) become dominant up to about 8 km.

The result from Fig. 3 is in contrast to the previous observation that average upward convective motions peak higher in the atmosphere than downward motions (Schumacher et al. 2015). This discrepancy may be due to the fact that midpoints of draft locations are shown in Fig. 3 instead of the full average convective motions from 0 to 15 km. An average velocity profile will be dominated by the strongest drafts, while Fig. 3 shows the distribution of draft locations in various lengths regardless of their strengths. Furthermore, upon investigating the
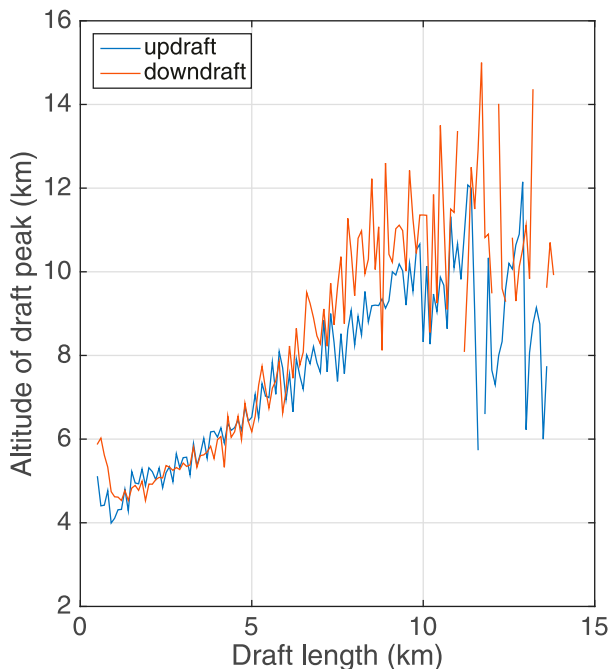

FIG. 4. The average altitude of draft peak (maximum velocity) associated with each draft length.

relationship between draft lengths and each of their associated average altitude of draft peaks, the peak altitudes of updrafts with lengths between 6 and 10 km are found to be lower than those of downdrafts (Fig. 4). Updrafts and downdrafts shorter than 6 km have similar peaking altitudes, while a difference is not clear for drafts longer than 10 km as their sample size is too small.

b. Averaged profiles

To examine the typical velocity profile within an updraft or downdraft for various length scales, the mean and median profile of the detected updrafts and downdrafts are shown in Figs. 5 and 6 for a range of size bins. Taking the average of the profiles in this way may lose information on features of individual profiles, such as any sharp increase or decrease in velocity, unless such features are occurring consistently at a particular point. It can, however, give us reliable insights about the general trend of velocity distribution, as the average is taken across numerous profiles.

Due to the way that our algorithm was set up, most profiles have a starting and ending mean velocity of around $1\,\mathrm{m\,s^{-1}}$ in magnitude for updrafts and $0.5\,\mathrm{m\,s^{-1}}$ for downdrafts. The maxima of updrafts are often located near the midpoint, with deviations up to ~1 km for longer drafts. Meanwhile for downdrafts of lengths 0.5–3 km, maxima are located near the midpoint or slightly below the midpoint. For downdrafts of 4 km or over in length, maxima are often located in the upper section, close to one-third of the way from the top. The mean velocities of updrafts in various length profiles are consistently higher than those of downdrafts, and updraft velocities also demonstrate a greater gradient, such that mean updrafts profile
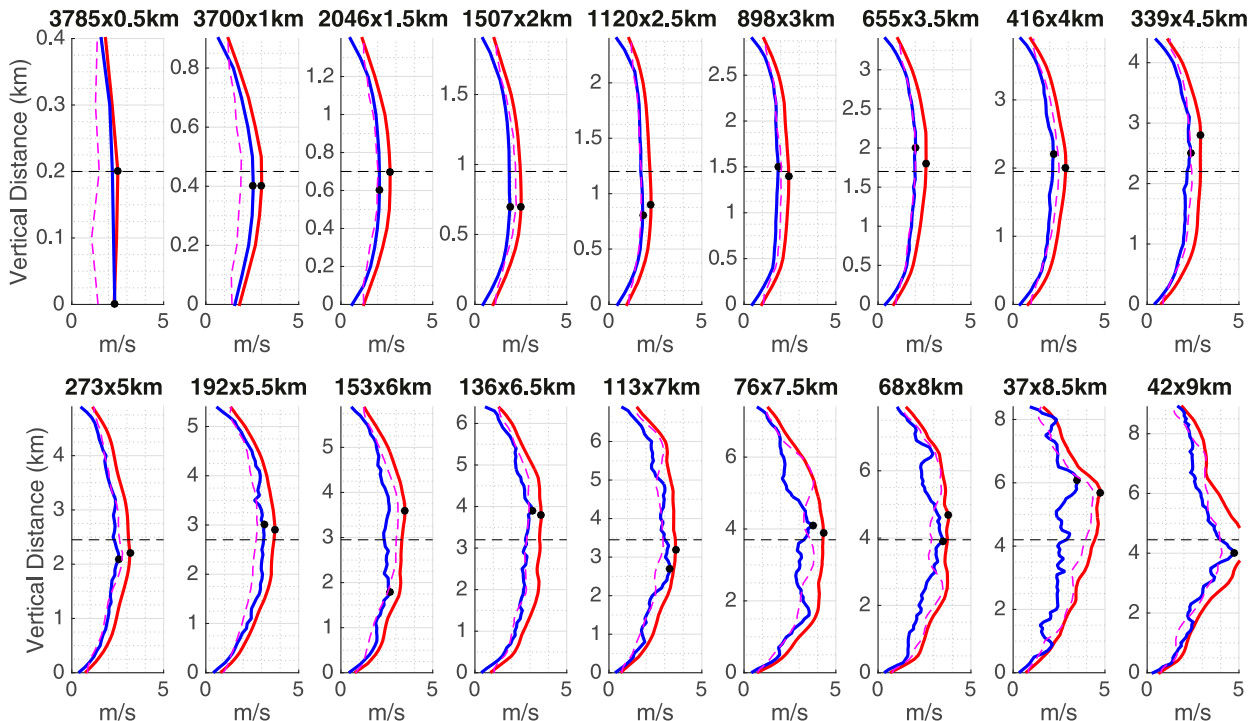
FIG. 5. Composite updraft profiles with lengths from 0.5 to 9 km, in increments of 0.5 km. Black dotted lines mark the midpoint of the updraft, and solid black circle marks the peak velocity. Solid red shows the mean, solid blue shows the median, and dashed magenta shows the standard deviation. The number of drafts going into each composite, and mean length, are shown at top of each panel.

is more "curved" than downdrafts. Having said that, updraft profiles have higher standard deviations and they consistently peak close to the midpoint. Furthermore, the peak velocity of updrafts scales up with its length, while the peak velocity of downdrafts is often at $\sim 2\,\mathrm{m\,s^{-1}}$.

c. Relationship with rain rates

To further investigate the characteristics of detected updrafts and downdrafts, rain rates derived from the 920-MHz reflectivity are discussed. Its conversion follows Eq. (1), and the rain rate associated with any detected draft has been averaged over ±30 min of the time of detection.

Statistics of rain rate for each height bin of updrafts/downdrafts are shown in Fig. 7. A positive relationship between rain rate and draft size is evident for both updrafts and downdrafts. The mean and median of rain rate become more inconsistent with increasing draft length, since the number of detected updrafts and downdrafts decreases exponentially with length, but in general the longer and deeper drafts produce higher rain rates, with almost a linear relationship albeit with significant scatter for larger drafts. This is true for drafts whose lengths are below ~ 10 km, as above which there is significant scatter and the sample size is small (Fig. 7).

Because the relationship between rain rate and draft length is noisy, and because rain rates are typically better known than draft sizes both in observations and large-scale models, it is worth examining the data the other way around by regressing draft lengths onto rain rate (Fig. 8). Naturally this confirms the

positive relationship seen before, but shows that the dependence of mean draft length on rain rate is relatively modest. The mean updraft length increases from about 2 km at low rain rates, to about 5–5.5 km at the highest rain rates. The 90th percentile changes more, from 4 km to about 10 km. Thus, the (rare) longest drafts tend to occur at high rain rates, but even the highest rain rates (20–30 mm h^{-1}) usually do not imply updrafts of more than 5-km length. Similar conclusions apply to downdrafts, whose mean length increases from roughly 2 km to about 3 km going from the lowest to highest rain rates.

d. Mass flux of updrafts

The average mass flux per draft of many drafts through the whole troposphere is $\langle \rho \omega H \rangle A / H_0$, where ρ is the density, ω the vertical velocity, H the draft length, A the cross-section area, and H_0 the depth of troposphere. By taking $\rho(z) \approx \rho_s \exp(-z/7.5)$, where ρ_s is the density at the surface and z the altitude (km), and assuming $\langle \rho \omega \rangle \approx \langle \rho \rangle \langle \omega \rangle$ if ω is not strongly varying, the fraction of total mass flux carried by a subset of updrafts, j, can be calculated using the following:

$$\frac{N_j}{N_{\mathrm{all}}} \frac{\langle \omega \rangle_j}{\langle \omega \rangle_{\mathrm{all}}} \frac{\langle H \rangle_j}{\langle H \rangle_{\mathrm{all}}} \exp\left(-\frac{\langle z \rangle_j - \langle z \rangle_{\mathrm{all}}}{7.5}\right), \qquad (2)$$

where N is the number of drafts.

Figure 9 shows the fraction of total mass flux carried by updrafts shorter than or equal to a certain length. It follows a
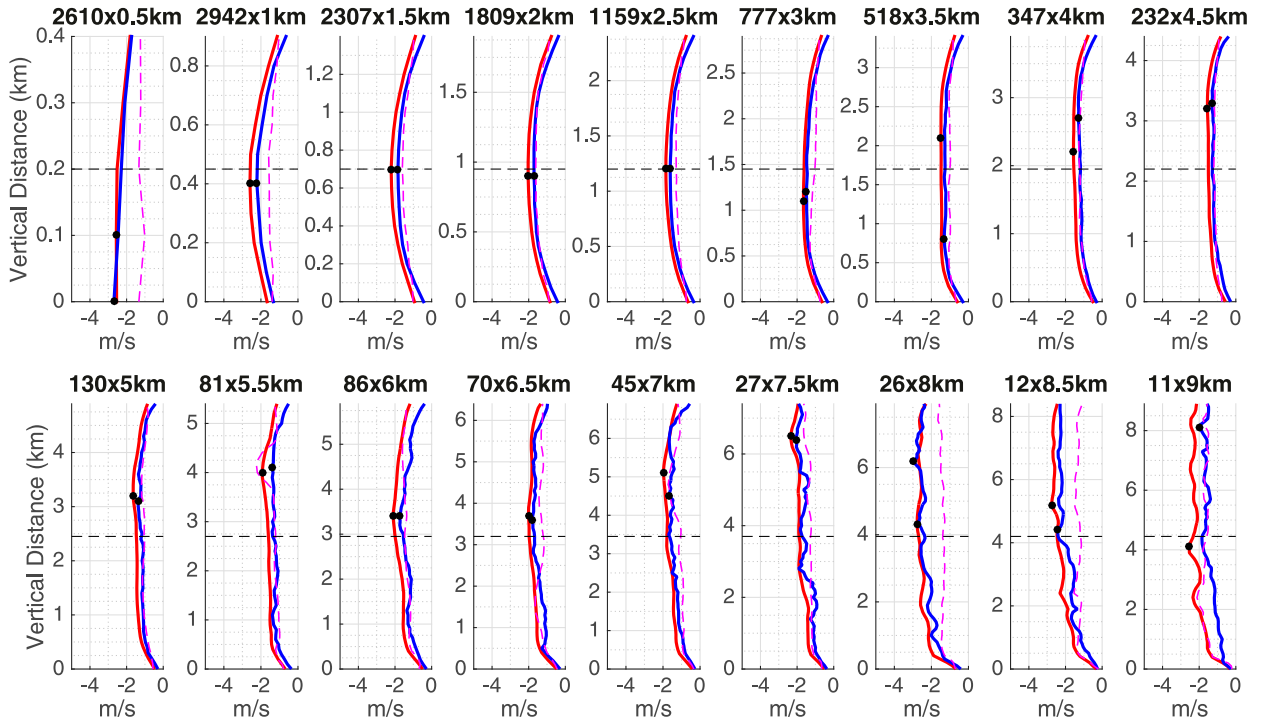
FIG. 6. As in Fig. 5, but for downdrafts.

nonlinear relationship, with the majority of total mass flux (~90%) carried by updrafts shorter than 8 km, and updrafts shorter than 3.2 km responsible for half of the total mass flux from all detected drafts. Even if the spikes dominated by small

updrafts seen in Fig. 3 are discarded as suspicious, the relationship (not shown) remains very close to what is shown in Fig. 9, such that half of the mass flux is still produced by updrafts shorter than 3.3 km.
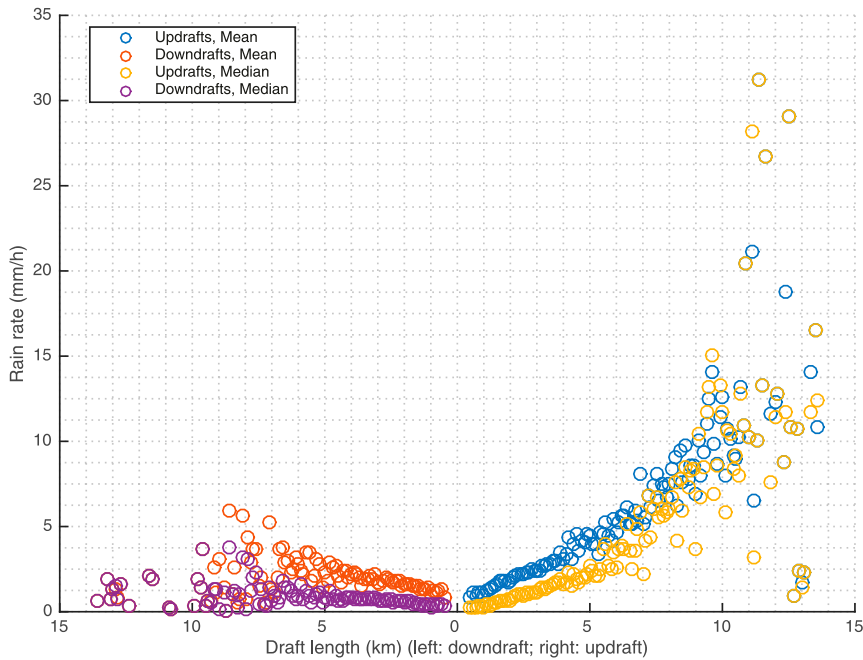

FIG. 7. Mean and median of derived rain rates against lengths of updrafts and downdrafts, starting from 500 m in increments of 100 m.
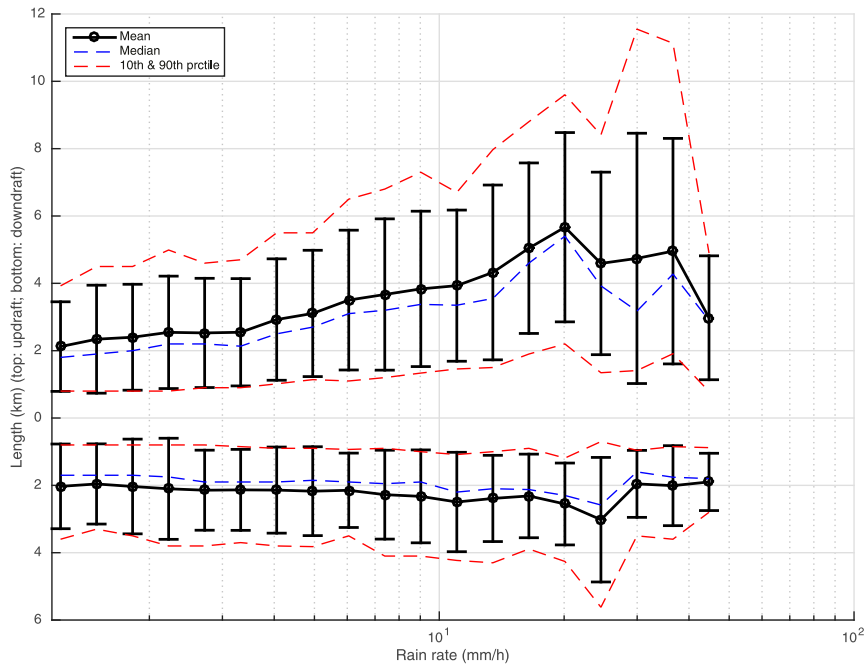
FIG. 8. (top) Updraft and (bottom) downdraft sizes binned by rain rate (where rain-rate bins scale logarithmically). Mean, median, 10%–90% percentile ranges, and one-sigma ranges about the mean are all shown.

4. Conclusions

We have compiled statistics of draft length in a dataset collected over roughly 1000 days during the rainy season in a tropical location, which spans over eight rainy seasons. The results appear broadly consistent with the conclusion from previous case studies, both numerically simulated and observed by radar, that most up- and downdrafts are quite small, though not as small as those found for isolated cumulus clouds in aircraft data Yang et al. (2016), and individual drafts spanning a majority of the troposphere are extremely rare. This study does not investigate the width, intensity, or duration of drafts.

We have explored the hypothesis suggested by case studies (particularly Dauhut et al. 2016) that strong, deep updrafts may finally appear when convection is sufficiently intense. We did this by stratifying the draft statistics by rain rate. Results confirm that drafts become longer at higher rain rates.

Since the sampling characteristics of our data are random, the upward mass flux per draft at any given level scales linearly with vertical velocity, and the frequency of occurrence of drafts at any given altitude scales with the overall number and vertical extents of drafts. The mean vertical velocity for drafts of greater than 5 km ($\sim 3.2\,\mathrm{m\,s^{-1}}$) is about 45% greater than for small drafts that are 1–1.5 km in length ($\sim 2.2\,\mathrm{m\,s^{-1}}$), and the former are roughly 3 times larger than the latter, but only 4712 out of the 61 376 drafts observed (7.7%) are greater than 5 km in length. Only 29% of the upward mass flux at any given level is carried by drafts greater than 5 km long (Fig. 9) (this percentage will be slightly higher in the midtroposphere and slightly lower toward the surface). At very high rain rates this

percentage will be higher. For drafts greater than 8 km, this percentage drops to 9%. In other words, ~71% of the upward mass flux is attributed to drafts smaller than 5 km.

The implication, that two-thirds of upward mass flux occurs in thermals or updrafts much less than half the troposphere in vertical extent, may explain previous findings that air in the upper troposphere has undergone substantial dilution, mixing, and/or delays in reaching the upper troposphere (Sherwood and Risi 2012; Luo et al. 2018). It suggests that massive updrafts
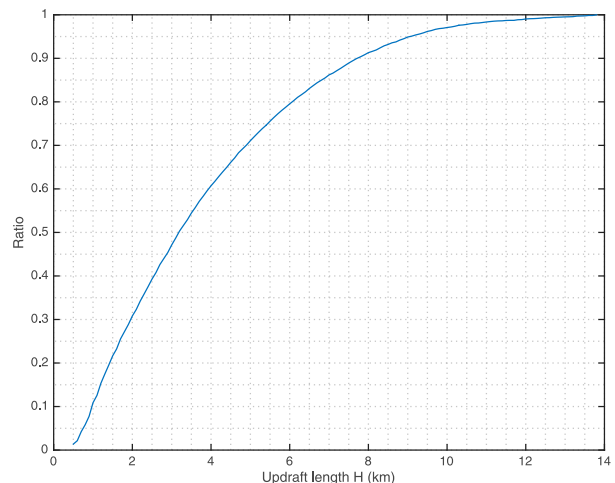

FIG. 9. Fraction of total mass flux of updrafts with length smaller than or equal to H out of all detected updrafts, calculated using Eq. (2).

of the type simulated in Hector by Dauhut et al. (2016) may not be the majority in convective systems, and that the near-absence of undilute ascent found in simulations of weakly organized convection is probably more typical. Even in the Hector case, huge numbers of small thermals were active throughout the troposphere well before the massive updrafts finally arrived. The relatively low occurrence of large drafts supports previous suggestions that a rethink of convective schemes used in global models may be in order, since most of these focus on deep, coherent, and often undilute plumes. As such, instead of assuming that they dominate in convective systems, we should consider a spectrum of draft sizes.

REFERENCES

Arakawa, A., 2004: The cumulus parameterization problem: Past, present, and future. *J. Climate*, **17**, 2493–2525, https://doi.org/10.1175/1520-0442(2004)017<2493:RATCPP>2.0.CO;2.

Blyth, A. M., W. A. Cooper, and J. B. Jensen, 1988: A study of the source of entrained air in Montana cumuli. *J. Atmos. Sci.*, **45**, 3944–3964, https://doi.org/10.1175/1520-0469(1988)045<3944:ASOTSO>2.0.CO;2.

——, S. G. Lasher-Trapp, and W. A. Cooper, 2005: A study of thermals in cumulus clouds. *Quart. J. Roy. Meteor. Soc.*, **131**, 1171–1190, https://doi.org/10.1256/qj.03.180.

Bryan, G. H., J. C. Wyngaard, and J. M. Fritsch, 2003: Resolution requirements for the simulation of deep moist convection. *Mon. Wea. Rev.*, **131**, 2394–2416, https://doi.org/10.1175/1520-0493(2003)131<2394:RRFTSO>2.0.CO;2.

Carpenter, R. L., K. K. Droegemeier, and A. M. Blyth, 1998: Entrainment and detrainment in numerically simulated cumulus congestus clouds. Part III: Parcel analysis. *J. Atmos. Sci.*, **55**, 3440–3455, https://doi.org/10.1175/1520-0469(1998)055<3440:EADINS>2.0.CO;2.

Carter, D. A., K. S. Gage, W. L. Ecklund, W. M. Angevine, P. E. Johnston, A. C. Riddle, J. Wilson, and C. R. Williams, 1995: Developments in UHF lower tropospheric wind profiling at NOAA's Aeronomy Laboratory. *Radio Sci.*, **30**, 977–1001, https://doi.org/10.1029/95RS00649.

Collis, S., A. Protat, P. T. May, and C. Williams, 2013: Statistics of storm updraft velocities from TWP-ICE including verification with profiling measurements. *J. Appl. Meteor. Climatol.*, **52**, 1909–1922, https://doi.org/10.1175/JAMC-D-12-0230.1.

Damiani, R., and G. Vali, 2007: Evidence for tilted toroidal circulations in cumulus. *J. Atmos. Sci.*, **64**, 2045–2060, https://doi.org/10.1175/JAS3941.1.

Dauhut, T., J.-P. Chaboureau, J. Escobar, and P. Mascart, 2016: Giga-LES of Hector the Convector and its two tallest updrafts up to the stratosphere. *J. Atmos. Sci.*, **73**, 5041–5060, https://doi.org/10.1175/JAS-D-16-0083.1.

Fierro, A. O., E. J. Zipser, M. A. LeMone, J. M. Straka, and J. Simpson, 2012: Tropical oceanic hot towers: Need they be undilute to transport energy from the boundary layer to the upper troposphere effectively? An answer based on trajectory analysis of a simulation of a TOGA COARE convective system. *J. Atmos. Sci.*, **69**, 195–213, https://doi.org/10.1175/JAS-D-11-0147.1.

French, J. R., G. Vali, and R. D. Kelly, 1999: Evolution of small cumulus clouds in Florida: Observations of pulsating growth. *Atmos. Res.*, **52**, 143–165, https://doi.org/10.1016/S0169-8095(99)00024-1.

Giangrande, S. E., S. Collis, J. Straka, A. Protat, C. Williams, and S. Krueger, 2013: A summary of convective-core vertical velocity properties using ARM UHF wind profilers in Oklahoma. *J. Appl. Meteor. Climatol.*, **52**, 2278–2295, https://doi.org/10.1175/JAMC-D-12-0185.1.

Hernandez-Deckers, D., and S. C. Sherwood, 2016: A numerical investigation of cumulus thermals. *J. Atmos. Sci.*, **73**, 4117–4136, https://doi.org/10.1175/JAS-D-15-0385.1.

Jackson, R., and Coauthors, 2021: The development of rainfall retrievals from radar at Darwin. *Atmos. Meas. Tech.*, **14**, 53–69, https://doi.org/10.5194/amt-14-53-2021.

Khairoutdinov, M., and D. Randall, 2006: High-resolution simulation of shallow-to-deep convection transition over land. *J. Atmos. Sci.*, **63**, 3421–3436, https://doi.org/10.1175/JAS3810.1.

Knupp, K. R., and W. R. Cotton, 1985: Convective cloud downdraft structure: An interpretive survey. *Rev. Geophys.*, **23**, 183–215, https://doi.org/10.1029/RG023i002p00183.

Kumar, V. V., C. Jakob, A. Protat, C. R. Williams, and P. T. May, 2015: Mass-flux characteristics of tropical cumulus clouds from wind profiler observations at Darwin, Australia. *J. Atmos. Sci.*, **72**, 1837–1855, https://doi.org/10.1175/JAS-D-14-0259.1.

Luo, Z. J., L. L. Pan, E. L. Atlas, S. M. Chelpon, S. B. Honomichl, E. C. Apel, R. S. Hornbrook, and S. R. Hall, 2018: Use of airborne in situ VOC measurements to estimate transit time spectrum: An observation-based diagnostic of convective transport. *Geophys. Res. Lett.*, **45**, 13 150–13 157, https://doi.org/10.1029/2018GL080424.

May, P. T., and D. K. Rajopadhyaya, 1999: Vertical velocity characteristics of deep convection over Darwin, Australia. *Mon. Wea. Rev.*, **127**, 1056–1071, https://doi.org/10.1175/1520-0493(1999)127<1056:VVCODC>2.0.CO;2.

Peters, J. M., H. Morrison, A. C. Varble, W. M. Hannah, and S. E. Giangrande, 2020: Thermal chains and entrainment in cumulus updrafts. Part II: Analysis of idealized simulations. *J. Atmos. Sci.*, **77**, 3661–3681, https://doi.org/10.1175/JAS-D-19-0244.1.

Protat, A., and C. R. Williams, 2011: The accuracy of radar estimates of ice terminal fall speed from vertically pointing Doppler radar measurements. *J. Appl. Meteor. Climatol.*, **50**, 2120–2138, https://doi.org/10.1175/JAMC-D-10-05031.1.

Riehl, H., and J. S. Malkus, 1958: On the heat balance in the equatorial trough zone. *Geophysica*, **6**, 503–537.

Romps, D. M., and Z. M. Kuang, 2010: Do undiluted convective plumes exist in the upper tropical troposphere? *J. Atmos. Sci.*, **67**, 468–484, https://doi.org/10.1175/2009JAS3184.1.

Rotunno, R., J. B. Klemp, and M. Weisman, 1988: A theory for strong, long-lived squall lines. *J. Atmos. Sci.*, **45**, 463–485, https://doi.org/10.1175/1520-0469(1988)045<0463:ATFSLL>2.0.CO;2.

Schumacher, C., S. N. Stevenson, and C. R. Williams, 2015: Vertical motions of the tropical convective cloud spectrum over Darwin, Australia. *Quart. J. Roy. Meteor. Soc.*, **141**, 2277–2288, https://doi.org/10.1002/qj.2520.

Scorer, R. S., and F. H. Ludlam, 1953: Bubble theory of penetrative convection. *Quart. J. Roy. Meteor. Soc.*, **79**, 94–103, https://doi.org/10.1002/qj.49707933908.

Sherwood, S. C., and C. Risi, 2012: The HDO/H_2O relationship in tropospheric water vapor in an idealized "last-saturation"

model. *J. Geophys. Res.*, **117**, D19205, https://doi.org/10.1029/2012JD018068.

——, D. Hernandez-Deckers, M. Colin, and F. Robinson, 2013: Slippery thermals and the cumulus entrainment paradox. *J. Atmos. Sci.*, **70**, 2426–2442, https://doi.org/10.1175/JAS-D-12-0220.1.

Wang, D., S. E. Giangrande, K. A. Schiro, M. P. Jensen, and R. A. Houze Jr., 2019: The characteristics of tropical and midlatitude mesoscale convective systems as revealed by radar wind profilers. *J. Geophys. Res. Atmos.*, **124**, 4601–4619, https://doi.org/10.1029/2018JD030087.

Williams, C. R., 2012: Vertical air motion retrieved from dual-frequency profiler observations. *J. Atmos. Oceanic Technol.*, **29**, 1471–1480, https://doi.org/10.1175/JTECH-D-11-00176.1.

Xu, K. M., and D. A. Randall, 2001: Updraft and downdraft statistics of simulated tropical and midlatitude cumulus convection. *J. Atmos. Sci.*, **58**, 1630–1649, https://doi.org/10.1175/1520-0469(2001)058<1630:UADSOS>2.0.CO;2.

Yang, J., Z. Wang, A. J. Heymsfield, and J. R. French, 2016: Characteristics of vertical air motion in isolated convective clouds. *Atmos. Chem. Phys.*, **16**, 10 159–10 173, https://doi.org/10.5194/acp-16-10159-2016.

Yano, J. I., 2014: Basic convective element: Bubble or plume? A historical review. *Atmos. Chem. Phys.*, **14**, 7019–7030, https://doi.org/10.5194/acp-14-7019-2014.

Yuter, S. E., and R. A. Houze, 1995a: Three-dimensional kinematic and microphysical evolution of Florida cumulonimbus. Part I: Spatial-distribution of updrafts, downdrafts, and precipitation. *Mon. Wea. Rev.*, **123**, 1921–1940, https://doi.org/10.1175/1520-0493(1995)123<1921:TDKAME>2.0.CO;2.

——, and ——, 1995b: Three-dimensional kinematic and microphysical evolution of Florida cumulonimbus. Part II: Vertical mass-transport, mass divergence, and synthesis. *Mon. Wea. Rev.*, **123**, 1964–1983, https://doi.org/10.1175/1520-0493(1995)123<1964:TDKAME>2.0.CO;2.